Solar-Terrestrial Physics. 2024. Vol. 10. Iss. 4. P. 46–58. DOI: 10.12737/stp-104202406. © 2024 M.A. Chernigovskaya, K.G. Ratovsky, G.A. Zherebtsov, A.G. Setov, D.S. Khabituev, A.S. Kalishin, A E. Stepanov, A.Yu. Belinskaya, V.V. Bychkov, S.A. Grigorieva,V.A. Panchenko. Published by INFRA-M Academic Publishing House

DOI: 10.12737/stp-104202406

Received April 25, 2024
Accepted July 02, 2024

IONOSPHERIC RESPONSE OVER THE HIGH AND MIDDLE LATITUDE REGIONS OF EURASIA ACCORDING TO IONOSONDE DATA DURING THE SEVERE MAGNETIC STORM IN MARCH 2015

M.A. Chernigovskaya
Institute of Solar-Terrestrial Physics SB RAS, Irkutsk, Russia, cher@iszf.irk.ru

K.G. Ratovsky
Institute of Solar-Terrestrial Physics SB RAS, Irkutsk, Russia, ratovsky@iszf.irk.ru

G.A. Zherebtsov
Institute of Solar-Terrestrial Physics SB RAS, Irkutsk, Russia, gaz@iszf.irk.ru

A.G. Setov
Institute of Solar-Terrestrial Physics SB RAS, Irkutsk, Russia, setov@iszf.irk.ru

D.S. Khabituev
Institute of Solar-Terrestrial Physics SB RAS, Irkutsk, Russia, Khabituev@iszf.irk.ru

A.S. Kalishin
Arctic and Antarctic Research Institute, St. Petersburg, Russia, askalishin@aari.ru

A.E. Stepanov
Yu.G. Shafer Institute of Cosmophysical Research and Aeronomy SB RAS, Yakutsk, Russia, a_e_stepanov@ikfia.sbras.ru

A.Yu. Belinskaya
Trofimuk Institute of Petroleum Geology and Geophysics SB RAS, Novosibirsk, Russia, belinskayaay@ipgg.sbras.ru

V.V. Bychkov
Institute of Cosmophysical Researches and Radio Wave Propagation of the FEB RAS, Paratunka, Russia, vasily.v.bychkov@gmail.com

S.A. Grigorieva
Institute of Geophysics UB RAS, Ekaterinburg, Russia, ion@arti.igfuroran.ru

V.A. Panchenko
Pushkov Institute of Terrestrial Magnetizm Ionosphere and Radio Wave Propagation RAS, Moscow, Russia, panch@izmiran.ru

Abstract. We have analyzed spatial and temporal variations in ionospheric parameters over high and middle latitudes of Eurasia, using data from chains of high- and mid-latitude ionosondes during a severe magnetic storm in March 2015. To analyze the ionospheric response to the severe geomagnetic disturbance of solar cycle 24, we have employed ionosonde data on hourly average values of the critical frequency f_oF2 of the ionospheric F2 layer, the critical frequency of the sporadic layer f_oE$_s$, and the minimum reflection frequency f_{min}. There are strong latitudinal and longitudinal differences between the features of temporal variations in the analyzed ionospheric parameters both under quiet conditions before the magnetic storm onset and during the storm.

We discuss possible causes of the observed spatial variations in ionospheric parameters. The source of spatio-temporal variations in ionospheric ionization parameters may be inhomogeneities generated in the high-latitude ionosphere under conditions of increased helio-geomagnetic activity. During the magnetic storm main and recovery phases, periods of blackouts of radio signals from ionosondes were observed at both high and middle latitudes. During these periods, there was a significant increase in the absorption of radio waves used in ionosonde sounding, as well as in the frequency of occurrence of screening sporadic E$_s$ layers. The long-term effect of the negative ionospheric storm over high and middle latitudes of Europe is explained by the movement of the vast region of the reduced density ratio [O]/[N2] at thermosphere heights from the Far East and Siberia westward to Europe during the late recovery phase of the magnetic storm. Increased ionization of the ionospheric F2 layer with f_oF2 exceeding the level for quiet days before the onset of the magnetic disturbance over the vast region of Eastern, Western Siberia and Eastern Europe after the end of the magnetic storm in March 2015 is a manifestation of the aftereffect of magnetic storms. The increase in ionization was especially pronounced, as measured by the chain of mid-latitude ionosondes.

Keywords: high- and mid-latitude ionosphere, ionosonde chain, geomagnetic storm, variations in ionosphere ionization, variations in thermosphere composition.

INTRODUCTION

This work is sequel to the studies of spatio-temporal variations in the ionization of the ionosphere of the Northern Hemisphere under quiet and disturbed geomagnetic conditions, which were based on data from chains of Eurasian ionosondes, GPS/GLONASS receivers, and INTERMAGNET magnetometers [Chernigovskaya et al., 2019, 2020, 2021]. For a comprehensive study into spatio-temporal features of ionospheric irregularities

from radiophysical measurement data, we add measurement data from a chain of high-latitude ionosondes, located at the latitude of the Arctic Circle (~66.5°) and higher latitudes of Eurasia, to the analysis. The first analysis of longitude-time variations in the maximum electron density over Eurasia have been carried out by analyzing data from the chain of high-latitude ionosondes during severe magnetic storms of solar cycle 24 in March and June 2015 in [Chernigovskaya et al., 2024].

Simultaneous analysis of measurement data from the mid- and high-latitude ionosonde chains will allow us to explore the global nature of spatio-temporal variations in ionospheric parameters over Eurasia, to delve into the similarities and differences between responses of the mid- and high-latitude ionosphere to variations in external (helio-geomagnetic activity) and internal (variations in the main geomagnetic field (GMF)) factors affecting ionospheric plasma. Studying time variations in longitude-latitude distributions of ionization parameters over the analyzed region of Eurasia will make it possible to examine the dynamics of expansion and motion of ionospheric ionization troughs from high to middle latitudes during magnetic storms.

This study focuses on variations in the parameters characterizing conditions of the high- and mid-latitude ionosphere during the severe magnetic storm of solar cycle 24 in March 2015. According to the classification [Hunsucker, Hargreaves, 2003] that divides the ionosphere into latitudinal zones with significantly different properties depending on geomagnetic latitude, by the mid-latitude ionosphere we mean geomagnetic latitudes 30°<*Glat*<60°. The high-latitude ionosphere includes *Glat*>60°). This region covers the subauroral ionosphere adjacent to it from midlatitudes (55°<*Glat*<65°) [Mamrukov et al., 2000], the auroral ionosphere (65°<*Glat*<75°), and the polar cap (*Glat*>75°).)

The high-latitude ionosphere has a complex spatial structure determined by its close relationship with Earth's magnetosphere and the processes occurring in it. Precipitation of high-energy charged particles from the magnetosphere into the ionosphere, intense electric fields and currents are among the main mechanisms for the formation of various large-scale structural features and irregularities in the high-latitude ionosphere. According to ground-based and satellite ionospheric sounding data, the following structural features of the high-latitude ionosphere have been identified: ionospheric ionization troughs (main, narrow, ring, high-latitude, etc.), polar and auroral ionization peaks, polar cavity, ionization tongue [Krinberg, Tashchilin, 1984; Deminov, 2015; Tumanova et al., 2016; Deminov, Shubin, 2018; Karpachev et al., 2019; Karpachev, 2019; Karpachev, 2021]. All these structural features have characteristic spatial and temporal peculiarities of formation, depend on helio-geomagnetic activity, time of year, time of day, geographical location of the observation site. They are most clearly manifested in winter or at night even under quiet geomagnetic conditions. In summer, when the high-latitude ionosphere is sunlit all day long (or most of the day) under polar day conditions, these features are smoothed out or absent altogether. The ionization troughs localized under quiet conditions in narrow latitudinal regions expand and shift to midlatitudes during increased geomagnetic activity. Neutral winds are induced in the high-latitude region, which redistribute the neutral atmospheric composition over most of the high-latitude region and part of the mid-latitude region. This eventually leads to changes in the rates of ionospheric plasma ionization and recombination. Furthermore, wind variations themselves are sources of ionospheric disturbances.

Inclusion of the high-latitude ionosphere having the unsteady and heterogeneous structure in the analysis is of particular fundamental importance for understanding physics of ionospheric processes in quiet and disturbed geomagnetic conditions, as well as for practical problems of ensuring stable radio communications and navigation in polar regions.

EXPERIMENTAL MEASUREMENT DATA

To analyze the spatio-temporal variations in ionospheric parameters during the severe geomagnetic disturbance in March 2015, we have used data on hourly average (or hourly for Parus ionosondes with 1 hr resolution) f_oF2, f_oE$_s$, and f_{min} from measurements of mid- and high-latitude Eurasian ionosonde chains. The high–latitude chain consists of seven ionosondes located in 67° – 71° N (58° N<*Glat*<65° N) in 26°–171° E in Eurasia (Figure 1, *a*, red marks and labels; Table 1). The chain contains ionosondes of ISTP SB RAS and SHICRA SB RAS — DPS-4 at the stations Norilsk, Zhigansk, as well as of AARI Roshydromet — CADI [MacDougall et al., 1995; Vystavnoy et al., 2013; Kalishin et al., 2020] at the stations Lovozero, Amderma, Salekhard, and Pevek. We also employ data from ionosonde SO166 (Alpha Wolf) [Kozlovsky et al., 2013; Enell et al., 2016] of Sodankylä Geophysical Observatory (Finland). Unfortunately, during the initial and main phases of the March 2015 storm the ionosonde in Amderma did not work for technical reasons. It was put back into operation on March 21 at 13:55 UT during the late recovery phase of the magnetic storm.

The mid-latitude chain consists of 8 ionosondes located in 50°–60° N (42°<*Glat*<54° N) in 13°–158° E (see Figure 1, *a*, white marks and labels; Table 2). The chain includes AIS ionosondes (IKIR FEB RAS, Paratunka), two Russian ionosondes Parus of various modifications (IPGG SB RAS, Novosibirsk; IGP UB RAS, Ekaterinburg) [Krasheninnikov et al., 2010], and five digital ionosondes DPS-4 of various modifications (SHICRA SB RAS, Yakutsk; ISTP SB RAS, Irkutsk; IZMIRAN, Moscow; Juliusruh, Průhonice) [Reinisch et al., 1997].

Before the onset of the magnetic storm on March 15–16, the ionosonde in Juliusruh did not work.

By mutual agreement between the study participants, all ionograms for the analyzed dates were processed manually in order to minimize possible errors during automated ionogram processing. As in previous studies based on measurements of the mid-latitude ionosonde chain [Chernigovskaya et al., 2019, 2020, 2021], we use f_oF2 proportional to the F-region maximum elec-

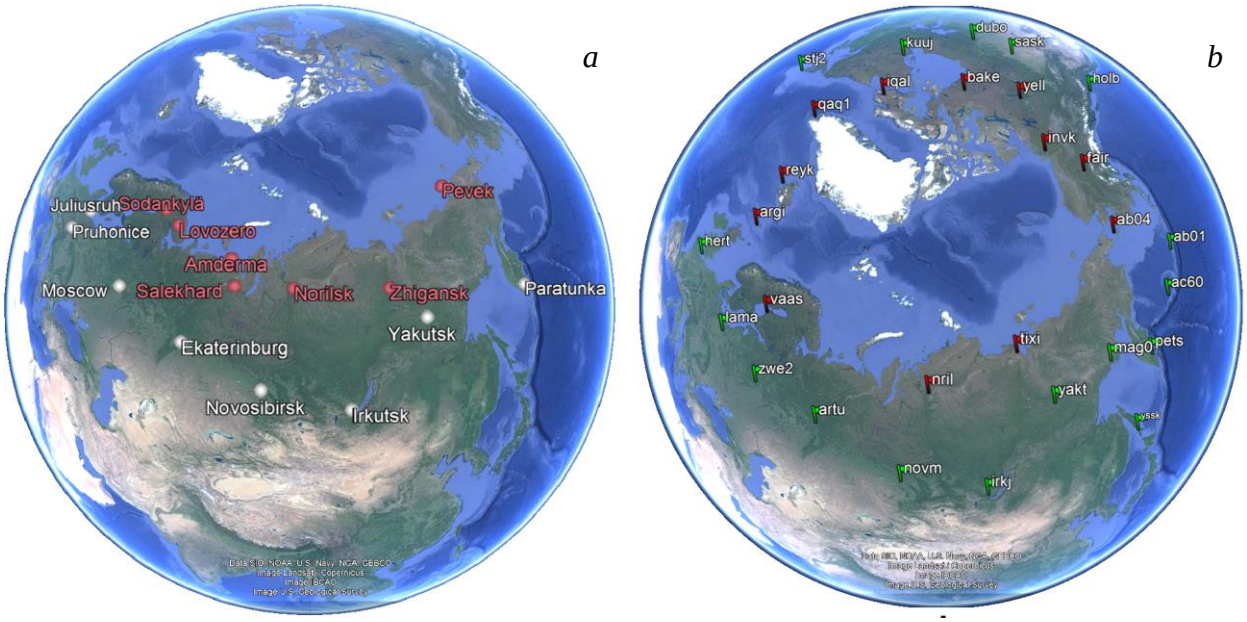

Figure 1. Layout of chains of ionosondes (*a*) and GPS/GLONASS receivers (*b*)

Table 1

Ionosondes of the high-latitude chain

Ionosonde	Ionosonde type	Geographic coordinates		Geomagnetic coordinates	
		latitude	longitude	latitude	longitude
Sodankylä	SO166	67° N	26° E	64° N	118° E
Lovozero	CADI	68° N	35° E	64° N	126° E
Amderma	CADI	70° N	61° E	63° N	147° E
Salekhard	CADI	67° N	67° E	59° N	150° E
Norilsk	DPS-4	69° N	88° E	60° N	166° E
Zhigansk	DPS-4	67° N	123° E	58° N	169° W
Pevek	CADI	71° N	171° E	65° N	135° W

Table 2

Ionosondes of the mid-latitude chain

Ionosonde	Ionosonde type	Geographic coordinates		Geomagnetic coordinates	
		latitude	longitude	latitude	longitude
Juliusruh	DPS-4D	55° N	13° E	54° N	99° E
Průhonice	DPS-4D	50° N	15° E	49° N	99° E
Moscow	DPS-4	56° N	37° E	52° N	122° E
Ekaterinburg	Parus 3.0	57° N	60° E	50° N	141° E
Novosibirsk	Parus 1.0	55° N	83° E	50° N	160° E
Irkutsk	DPS-4	52° N	104° E	42° N	177° E
Yakutsk	DPS-4	62° N	130° E	53° N	163° W
Paratunka	AIS	53° N	158° E	46° N	138° W

tron density N_mF2 to analyze magnetic storm effects in N_mF2 variations [Polyakov et al., 1968]. The time resolution for different ionosondes varies from 15 min to 1 hr (for Parus ionosondes). Gaps in the time series of ionosonde measurements were replaced by linear interpolation of adjacent available measurements.

RESULTS OF ANALYSIS OF EXPERIMENTAL DATA ON IONIZATION OF THE HIGH- AND MID-LATITUDE IONOSPHERE OVER EURASIA AND THEIR DISCUSSION

Features of the most intense magnetic storm in solar cycle 24 on March 17–19, 2015 has been thoroughly analyzed in [Chernigovskaya et al., 2019, 2020, 2021, 2024]. According to the classification of storms by the planetary index *Dst* [Loewe, Prölss, 1997], this storm was classified as very strong, severe (*Dst*<–200 nT). According to NASA's classification based on the K_p index, the storm was classed as G4 [https://www.swpc.noaa.gov/noaa-scales-explanation]. At the moment of maximum intensity on March 17 at 22:47 UT, *Dst* dropped to –223 nT.

During magnetic storms, a broad range of complex processes (ionospheric storms) develop in the ionosphere, which alter its parameters significantly. During geomagnetic disturbances, f_oF2 can decrease or increase as compared to quiet conditions (negative or positive ionospheric storms respectively) [Matsushita, 1959; Buonsanto, 1999; Mikhailov, 2000].

Top panels in Figure 2 illustrate longitude-time variations in f_oF2 as measured by the high- (*a*) and mid-latitude (*b*) Eurasian ionosonde chains for March 15–25. Variations in *Dst* during the magnetic storm are shown below.

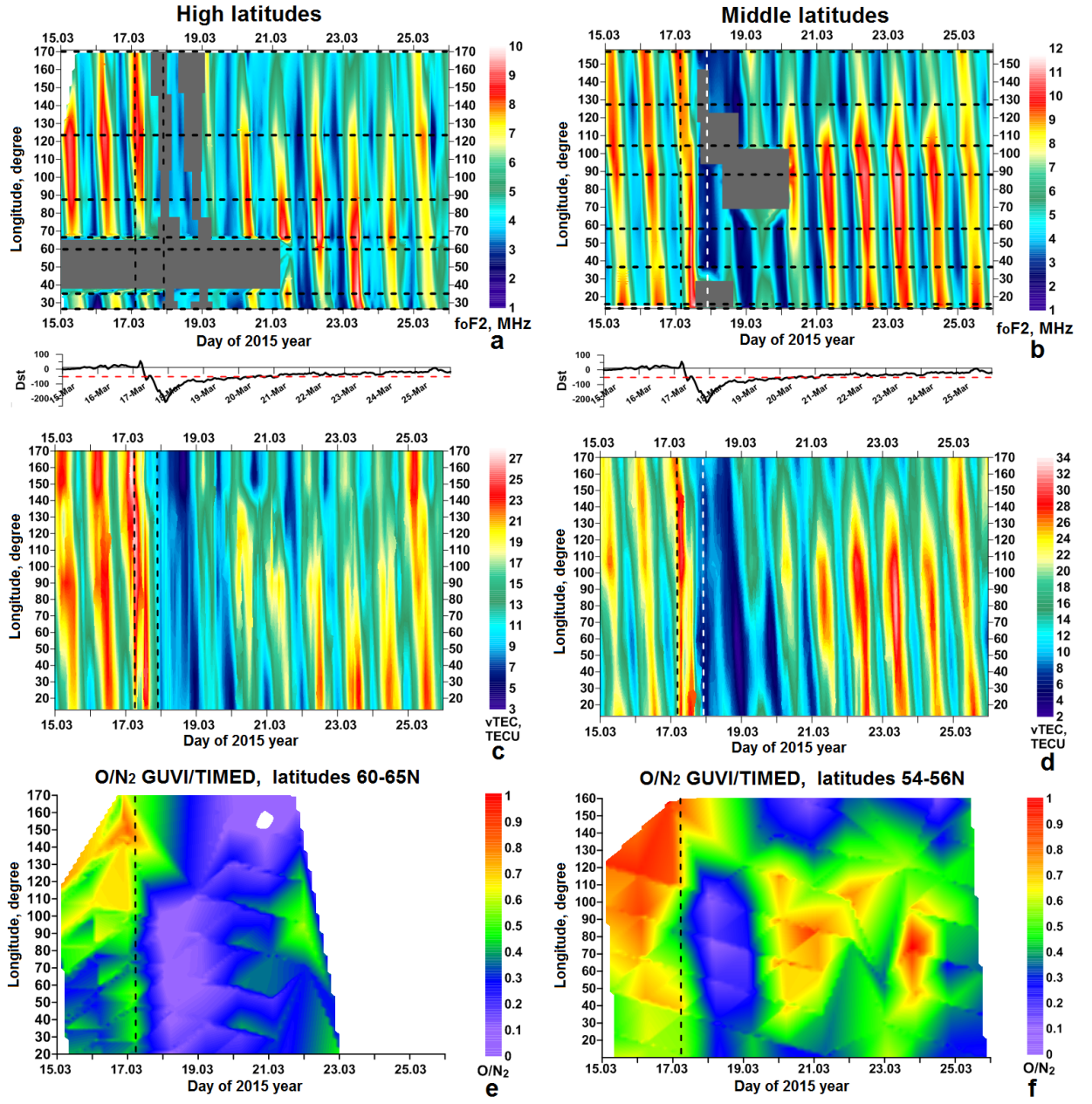

Figure 2. Longitude-time variations in f_oF2 according to data from high- (*a*) and mid-latitude (*b*) Eurasian ionosonde chains; TEC variations according to data from high- (*c*) and mid-latitude (*d*) chains of GPS/GLONASS receivers [Chernigovskaya et al., 2020, 2021]; longitude-time distributions of [O]/[N_2] as measured by GUVI TIMED for high (*e*) and middle (*f*) latitudes in March 2015 (UT)

The red dashed line denotes the level starting from which at $Dst \leq -50$ nT the geomagnetic disturbance conditions are classified as stormy according to the classification [Loewe, Prölss, 1997]. Vertical dashed lines indicate the sudden commencement of the magnetic storm. Gray rectangles mark periods of data absence due to technical reasons or periods of blackouts of ionosonde radio signals.

Including measurement data from the high-latitude Eurasian ionosonde chain in the analysis has made it possible to compare the longitude-time variations in N_mF2 over high and middle latitudes of Eurasia (*a*, *b*) with similar variations in the total electron content (TEC) (*c*, *d*) obtained from measurements carried out at high- and mid-latitude chains of dual-frequency GPS/GLONASS phase receivers (see Figure 1, *b*) [Chernigovskaya et al., 2020, 2021]. Panels *a*–*d* in Figure 2 are in fairly good qualitative agreement. Reasons for possible discrepancies are discussed in detail in [Perevalova et al., 2023; Chernigovskaya et al., 2023]. From the analysis of Figure 2 we can confidently state that there are longitude differences between N_mF2 and TEC variations both at high (*a*, *c*) [Chernigovskaya et al., 2024] and middle (*b*, *d*) latitudes [Chernigovskaya et al., 2019, 2020, 2021].

When comparing N_mF2 over Eurasia at high (*a*, *c*) and middle (*b*, *d*) latitudes, first of all noteworthy are the differences in the general level of f_oF2 and in the diurnal variations under quiet conditions (before the storm) at the equinox. This is explainable and understandable due to the difference in the sunlit conditions between high and middle latitudes of the Northern Hemisphere in the spring equinox season. With increasing magnetic activity (in the conditions of ionospheric storm development), the f_oF2 and TEC variabilities in the high-latitude ionosphere are also lower than at mid-latitudes, even in the case of such a severe magnetic storm. Similar effects in the ionosphere at different latitudes were observed in [Araujo-Pradere et al., 2005].

Figure 3 additionally illustrates time variations in f_oF2 for each ionosonde as measured at high- (*a*) and mid-latitude (*b*) Eurasian ionosonde chains for March 15–25 (points in the plots). Vertical dashed lines indicate the moment of the storm sudden commencement (S) and the moment of maximum intensity of the magnetic storm (M) for *Dst* variations (bottom panels). Solid horizontal lines show daily average f_oF2 calculated for 14 quiet days before the storm commencement. Gray rectangles in Figure 2, *a*, *b* mark the periods of absence of ionosonde measurement data.

The storm main phase lasted ~16.5 hrs — from the storm sudden commencement (SSC) at 06:23 UT (S lines in Figure 3) to 22:47 UT on March 17. At the maximum of the storm, *Dst* decreased to –223 nT (M lines in Figure 3). After SSC in the first half of March 17, the effect of a positive ionospheric storm was detected both by the ionosondes (see Figure 2, *a*, *b*) and by GPS/GLONASS receivers (see Figure 2, *c*, *d*). According to data from the ionosondes in Ekaterinburg, Moscow, Průhonice, and Juliusruh (Figure 2, *b*, 3, *b*), as well as according to TEC data (Figure 2, *d*), a particularly strong increase in the electron density was observed over the mid-latitude region of Europe. From the second half of March 17, f_oF2 began to decrease sharply. According to data from high-latitude ionosondes in Pevek, Zhigansk, and Salekhard, there were complete blackouts of radio signals (Figures 2, *a*, 3, *a*). According to data from high-latitude ionosondes (Figures 2, *a*, 3, *a*) in Norilsk, Lovozero, and Sodankylä with short intervals of blackouts during the storm main phase on March 17, it is still possible to trace diurnal variations of f_oF2. According to data from mid-latitude ionosondes (Figures 2, *b*, 3, *b*), from the second half of March 17 complete blackouts of radio signals were recorded in Průhonice (for a day); a little later and less prolonged, in Yakutsk and Irkutsk. The decrease in f_oF2 at midlatitudes coincides with the *Dst* minimum (Figures 2, *b*, *d*, 3, *b*), which is associated with the expansion of the magnetospheric convection zone from high to middle latitudes. Plasma motion induced by a large-scale electric field (**E**×**B** drift) causes part of the plasmasphere to empty out and the plasmapause to shift to Earth, i.e. by smaller *L* (*L* is the distance to the top of the field line in Earth radii). Ionospheric plasma rises, reducing the electron density and hence f_oF2. Such a scenario of ionospheric storm development with a change of positive and negative effects is typical for the equinox season and is most pronounced in the mid-latitude ionosphere [Burešová et al., 2007; Ratovsky et al., 2020].

After reaching the maximum intensity of the magnetic storm (M line in Figure 3) in the early recovery phase, there is a further decrease in f_oF2. This is clearly seen from the location of the points in the plots of variations relative to daily average f_oF2 under quiet conditions (solid horizontal lines). During March 18–19, the recorded values of f_oF2 were lower than daily average f_oF2 under quiet conditions by more than 2 MHz for ionosondes in Zhigansk and Norilsk (see Figure 3, *a*). Large gaps in data were observed for ionosondes in Salekhard, Lovozero, and Sodankylä on March 18–19 (Figure 3, *a*), it is therefore impossible to determine how much f_oF2 changed. The periods of complete radio signal blackout occurred at night when the probability of formation of ionization troughs is high (Figures 2, *a*, 3, *a*). For the highest-latitude ionosonde in Pevek, the period of decreased f_oF2 and hence N_mF2 lasted almost until March 24 inclusive, with a small burst of f_oF2 on March 19 (see Figure 3, *a*). A sharp decrease in the electron density was observed at high latitudes and in data on vertical TEC (see Figure 2, *c*).

The development of a strong negative ionospheric storm during the magnetic storm recovery phase in the period after March 18 was also recorded in data from the chain of mid-latitude ionosondes (Figures 2, *b*, 3, *b*) and GPS/GLONASS receivers (Figure 2, *d*). A sharp drop in f_oF2 by 5 MHz or more relative to daily average f_oF2 in quiet conditions was noted for ionosondes in Paratunka (to March 24 inclusive), Yakutsk (to March 21 inclusive), Irkutsk, Ekaterinburg, Moscow, Juliusruh (to March 19 inclusive), and

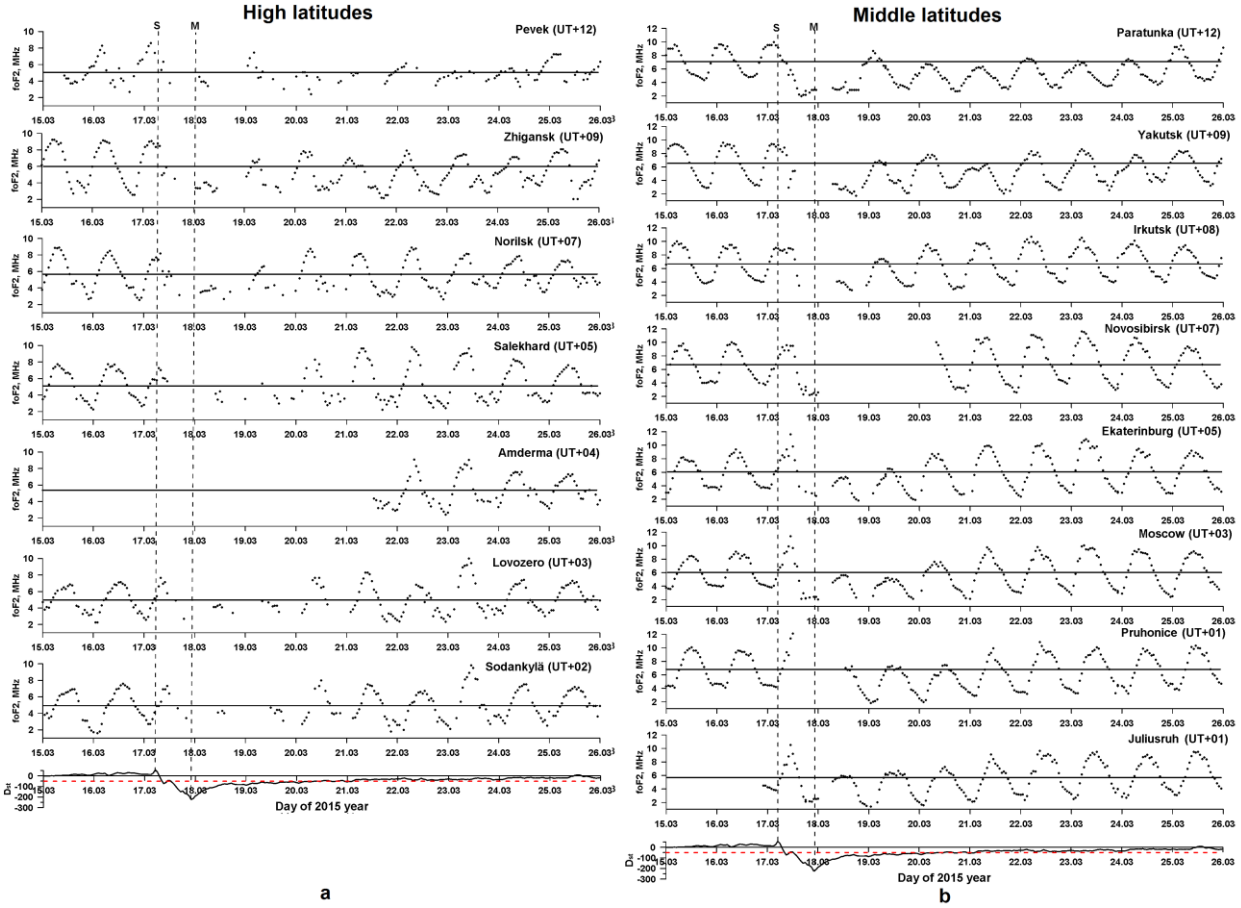

Figure 3. Time variations in f_oF2 (dots) as measured by ionosondes of high- (*a*) and mid-latitude (*b*) chains and variations in *Dst* (UT). Vertical dashed lines indicate the storm commencement (S) and the maximum intensity (M). Solid horizontal lines are daily average levels of f_oF2 under quiet geomagnetic conditions

and Průhonice (to March 20 inclusive). The ionosonde in Novosibirsk didn't operate for two days from March 18 to March 20. During the early recovery phase of the magnetic storm on March 18 (Figure 3, *b*), the f_oF2 values were very low (2–4 MHz) at longitudes 80°–120° E over the Far East and Siberia. Ionosondes in Novosibirsk, Irkutsk, Yakutsk, and Paratunka were inside the auroral ionospheric trough whose southern boundary shifted deep to midlatitudes. Typical auroral ionograms were recorded in all these ionosondes [Chernigovskaya et al., 2021]. From March 20, daily N_mF2 (Figure 2, *b*) and TEC (Figure 2, *d*) in the Siberian longitude sector (Novosibirsk, Irkutsk) began to recover to undisturbed levels, whereas over Eastern Europe in 30°–60° E daily variations in f_oF2 were still below the daily average level under quiet conditions (Figure 3, *b*). Unexpectedly, in the European sector the southern boundary of the auroral ionization trough shifted to ~55° N 2–3 days after the magnetic storm reached the maximum intensity on March 17. By March 20–21, the region of low electron density shifted to the European sector; and in Siberia, f_oF2 almost recovered to the undisturbed level (Figure 2, *b*, *d*). At Far Eastern longitudes 130°–160°, the electron density of the ionosphere, which began to recover on March 19, decreased again on March 20–21 below the daily average level under quiet conditions and remained so, according to the ionosonde in Paratunka, almost until March 24 (Figure 3, *b*).

To explain the spatio-temporal variations in the ionospheric parameters during the storm, bottom panels in Figure 2 show longitude-time distributions of the density ratio $[O]/[N_2]$ in the atmospheric gas column in the thermosphere (ionosphere) above ~100 km for high-latitude 60°–65° N (Figure 2, *e*) and mid-latitude 54°–56° N (Figure 2, *f*) regions, as measured by the GUVI TIMED UV spectrometer [Christensen et al., 2003]. The distribution of $[O]/[N_2]$ in Figure 2, *e* for the high-latitude region is available only until March 22–23 to a maximum latitude ~65° N, probably due to the peculiarities of orbital inclination of the TIMED satellite. The physical parameter $[O]/[N_2]$ is a good indicator of negative phases of ionospheric storms [Prölss, Werner, 2002; Laštovička, 2002; Danilov, 2003; Liou et al., 2005]. The decrease in $[O]/[N_2]$ in the thermospheric gas causes the electron density to decrease in this region. Complex electrodynamic processes occurring under conditions of increased geomagnetic activity in polar latitudes lead to a strong decrease in $[O]/[N_2]$ in the thermosphere. Comparing f_oF2 variations at high and middle latitudes of the Eastern Hemisphere over Eurasia in the F2 layer (Figure 2, *a*, *b*) and ionospheric TEC (Figure 2, *c*, *d*) with variations of the neutral composition at the same latitudes and longitudes (Figure 2, *e*, *f*), we can note that they correlate quite well. Longitude-time distributions of

[O]/[N_2] well explain the previously described features of the ionospheric plasma response to severe geomagnetic disturbance: 1) a long-term dramatic decrease in f_oF2 in the high- and mid-latitude ionosphere over the Far East until March 24 according to data from ionosondes in Pevek (Figures 2, *a*, 3, *a*), Paratunka (Figures 2, *b*, 3, *b*), and ionospheric TEC (Figure 2, *c*, *d*); 2) recovery of the electron density in the ionosphere over high- and mid-latitude regions of Eastern and Western Siberia from March 20 according to data from the ionosondes in Norilsk, Salekhard (Figures 2, *a* and 3, *a*), Irkutsk, Novosibirsk (Figures 2, *b* and 3, *b*) and ionospheric TEC (Figure 2, *c*, *d*) earlier in comparison with the adjacent longitude regions of the Far East and Europe; 3) long-term effect of the negative ionospheric storm over the high- and mid-latitude European regions until March 21 when the recovery phase of the magnetic storm had already ended (see *Dst* variations in Figures 2 and 3). GMF is generally considered quiet when *Dst* > –20 nT.

The complete absence of traces of reflections of radio signals generated by ionosondes in ionograms results from the joint action of mechanisms for decreasing the electron density in the upper ionosphere (negative ionospheric storms are the dominant process in the ionospheric response to increased geomagnetic activity) and abnormally increasing radio wave absorption in the lower ionosphere. During severe disturbances associated with various phenomena on the Sun and in Earth's magnetosphere, the electron density in the lower ionosphere in the D-region (50–90 km) can increase tens or hundreds of times due to precipitation of energetic particles from the magnetosphere along geomagnetic field lines into the high-latitude ionosphere, which causes radio wave absorption to increase sharply [Mitra, 1977; Bryunelli, Namgaladze, 1988]. As a result, the mid- and high-frequency radio waves used in vertical sounding (VS) by ionosondes are completely absorbed in the lower ionosphere. This phenomenon is called blackout and seriously hinders ionospheric observations by traditional methods, in particular by vertical and oblique radio sounding. The f_{min} parameter is often utilized as a qualitative characteristic of radio wave absorption in the ionosphere [Mitra, 1977]. Radio wave propagation to h_mF2 can also be hindered by irregular thin layers about several kilometers thick with increased electron density, which appear in the E-region (90–140 km) — sporadic E_s layers. At high latitudes, especially during magnetic disturbances [Blagoveshchensky et al., 2017], these layers form quite often. They can have a significant effect on radio wave propagation by blocking the overlying ionospheric layers. Along with the increase in attenuation in the D layer during geomagnetic disturbances, this can lead to complete absorption of radio signals.

Therefore, to analyze the effect exerted by a magnetic storm on the ionospheric electron density in more detail, it is necessary to additionally examine variations in f_{min} (Figures 4, *a*, *b*, 5, *a*, *b*) characterizing radio wave absorption in the lower ionosphere in the D-region, as well as in f_oE_s (Figure 4, *c*, *d*) describing the formation of screening E_s layers.

Figures 4, *a*, *b*, 5, *a*, *b* illustrate spatio-temporal variations in f_{min} — the minimum frequency from which a trace of reflections from the ionosphere is seen in the VS ionogram. In general, comparing time variations in f_oF2 (Figure 3, *a*, *b*) and f_{min} (Figure 5, *a*, *b*), we can argue that the periods of absence of f_oF2 data from ionosonde measurements are directly related to a significant increase in radio wave absorption in the lower ionosphere during the main phase and especially during the recovery phase of the severe magnetic storm in March 2015. There are significant differences between time (including daily) variations in f_{min} for high (Figures 4, *a*, 5, a) and middle (Figures 4, *b*, 5, *b*) latitudes, as well as significant longitude variations in f_{min}, recorded by ionosondes in one latitudinal region, but at different longitudes.

For high latitudes, daily average f_{min} under quiet conditions, as measured by all ionosondes, was ~2 MHz with ±1 MHz variations during the day with a maximum in the morning or afternoon and a minimum at night. During the magnetic storm main phase on March 17, f_{min} increased to 4 MHz. There were periods lasting several hours on March 17–18 when the ionosondes in Pevek and Zhigansk were completely out of operation. It was unexpected that the highest values of f_{min} were recorded during the magnetic storm recovery phase (see Figures 4, 5) according to data from ionosondes in Zhigansk (f_{min}=6.2 MHz in the morning on March 21), Norilsk (f_{min}~6 MHz in the afternoon on March 20, f_{min}=6.4 MHz in the morning on March 23), Salekhard (f_{min}=6 MHz in the afternoon on March 21), Lovozero (f_{min}~6 MHz in the morning on March 19, in the afternoon on March 20, f_{min}=6.7 MHz in the afternoon on March 21), and Sodankylä (f_{min}~6 MHz in the afternoon on March 20). Note that in the period after March 20, *Dst* was already above the storm level (the red dashed line of *Dst* in Figures 3, 5). Bursts of f_{min} and hence an enhancement in radio wave absorption in the lower ionosphere might have been related to an isolated burst of magnetic activity on March 22 from ~06 to 18 UT [Chernigovskaya et al., 2021, 2024]. The increase in activity was caused by the impact of coronal hole high-speed stream (CH HSS) on Earth's magnetosphere. Geomagnetic effects associated with CH HSS events usually have little effect on *Dst* variations, but are clearly visible in variations of other geomagnetic indices, especially *PCN*, *AE*, A_p, and K_p [Chernigovskaya et al., 2024]. All these indices increased significantly again on March 22. An increase in *AE* indicates directly an increase in magnetic activity in the polar zone due to amplification of ionospheric currents flowing along the auroral oval boundary. Such an enhancement in electrodynamic processes in the D- and E-regions in the auroral, subauroral, and adjacent mid-latitude regions, where the equatorial boundary of auroral ionization troughs shifts during periods of increased geomagnetic activity, may well be the cause of the observed strong variations in the ionospheric parameters of the lower ionosphere.

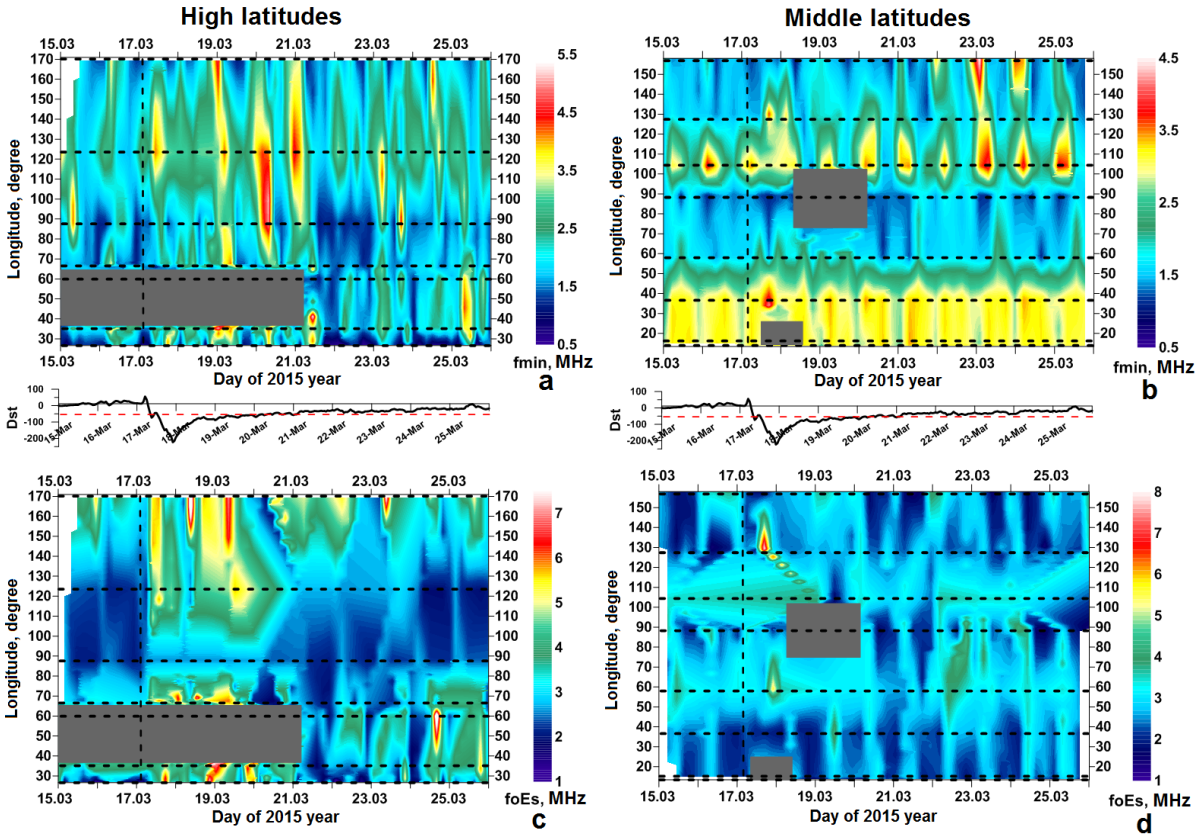

Figure 4. Longitude-time variations of f_{min} and f_oE_s according to data from high- (*a*, *c*) and mid-latitude (*b*, *d*) Eurasian ionosonde chains in March 2015 (time UT)

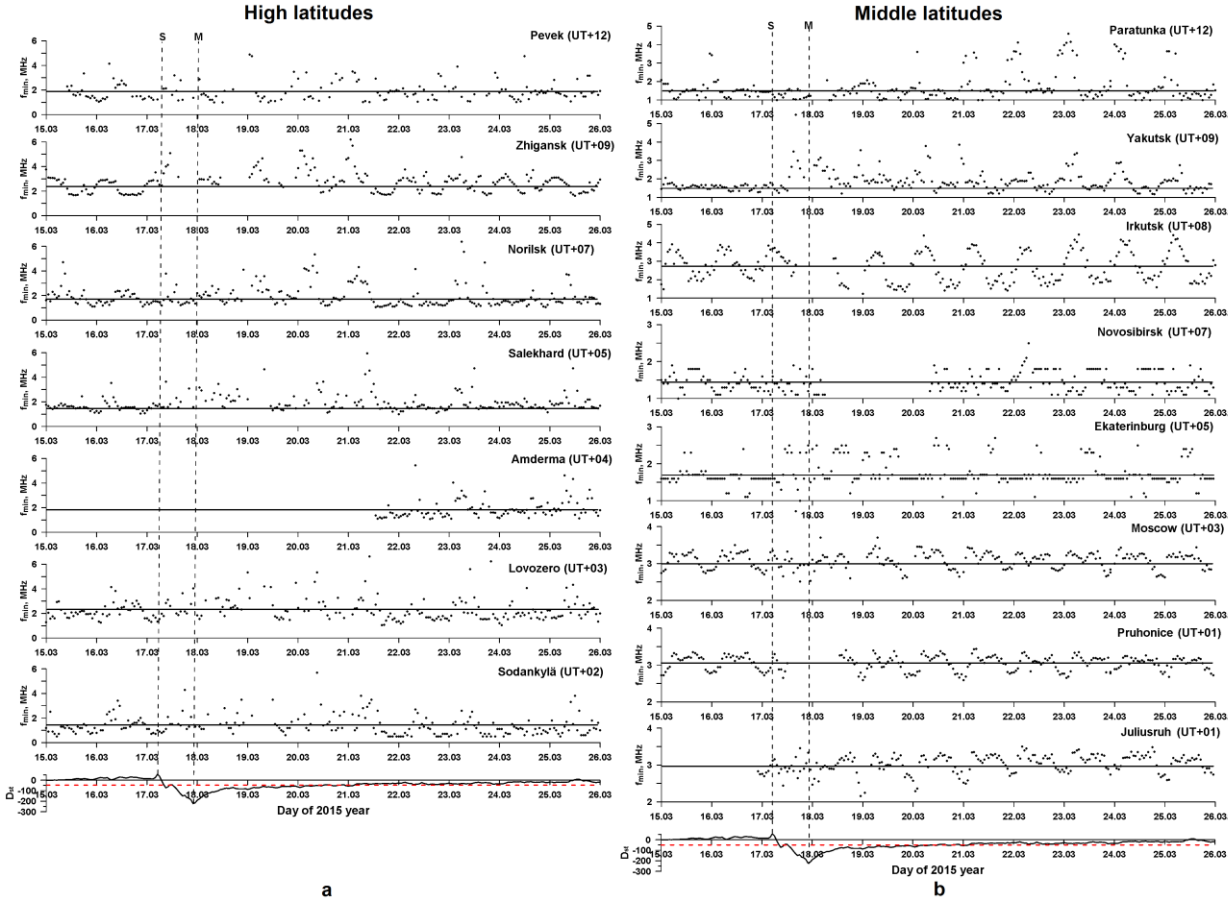

Figure 5. The same as in Figure 3 for f_{min}

For the mid-latitude region, daily average f_{min} in quiet conditions differ for different ionosondes. For the ionosondes in Paratunka, Yakutsk, Novosibirsk, and Ekaterinburg, daily average f_{min} was 1.6±05 MHz; for the ionosondes in Moscow, Průhonice, and Juliusruh, 3±05 MHz (Figures 4, *b* and 5, *b*). Especially noteworthy is the measurement data from the ionosonde in Irkutsk, where this value was 2.8±1 MHz. Such differences in the recorded ionospheric parameters can be explained, firstly, by the manifestation of regional longitude features of variations in the parameters of the lower ionosphere under quiet conditions; secondly, by technical differences between modifications of the ionosondes in use, as well as, possibly, of the technique for manual processing of VS ionograms to which the analyzed parameter f_{min} is very critical.

Diurnal variations in f_{min} (Figure 5, *b*) are similar to the observed diurnal variations at high latitudes (Figure 5, *a*) — with a maximum in the morning or afternoon and a minimum at night. With increasing geomagnetic activity during the magnetic storm main phase in the second half of March 17, f_{min} increased significantly even at night to 3 and even to 5 MHz according to the ionosonde in Yakutsk; to 2.5 MHz in Ekaterinburg; to 4 MHz in Moscow; and to 3.5 MHz in Juliusruh. There were periods lasting several hours on March 17–18 when the ionosondes were completely out of operation in Paratunka, Irkutsk, Novosibirsk (two days), and Průhonice (a little more than a day). But the highest values of f_{min} were recorded during the recovery phase of the magnetic storm (see Figures 4, *a*, 5, *b*) by the ionosondes in Paratunka on March 20–24, in Yakutsk on March 17–21 and 23–25, in Ekaterinburg on March 17–19 (Figure 5, *b*). During the same periods, as noted above, a sharp decrease in f_0F2 by 5 MHz or more was detected relative to the daily average level under quiet conditions for the ionosondes in Paratunka (to March 24 inclusive), Yakutsk (to March 21 inclusive), and Ekaterinburg (to March 19 inclusive) (see Figure 3, *b*).

During the magnetic storm considered, a high occurrence rate of E_s layers was recorded at both high (Figure 4, *c*) and middle (Figure 4, *d*) latitudes. A significant enhancement (to 8–9 MHz) in the formation of E_s layers over a very long period, which covered not only the main and recovery phases of the magnetic storm, but also the subsequent period until March 25, was observed in data from the highest-latitude ionosonde in Pevek. During the magnetic storm main and recovery phases on March 17–19, sporadic layers also formed very intensively in the E-region over high-latitude regions of Zhigansk, Salekhard, Lovozero, and Sodankylä (Figure 4, *c*), as well as over mid-latitude regions of Yakutsk and Ekaterinburg (Figure 4, *d*).

DISCUSSION OF THE ANALYSIS RESULTS

According to the results of previous studies [Chernigovskaya et al., 2019, 2020, 2021, 2023], the reason for the observed longitude irregularity of ionospheric ionization over Eurasia has first been attributed to the irregular structure of longitude variability of GMF components, which arises from spatial anomalies of various scales in the background main geomagnetic field. Using data from two chains of INTERMAGNET magnetometers at middle and high latitudes, longitude distributions of dispersions of the GMF *H* and *Z* components for the magnetic storm event considered under quiet conditions before the storm and under disturbed conditions during the development of the storm have been obtained [Chernigovskaya et al., 2019, 2020, 2021]. In the longitude distribution of GMF variations, pronounced longitudes have been identified at which the intensity of variations has maxima and minima. Maximum longitude variations in the dispersions are generally observed at midlatitudes (~55° N). At high latitudes (~70° N), the GMF variability is more uniform in longitude. During magnetically disturbed periods at midlatitudes of the Eastern Hemisphere over Eurasia, two zones of strong GMF variations are formed in longitude sectors near ~40° and ~130° E. They correspond to the regions of strong negative ionospheric disturbances, i.e., a decrease in f_0F2, which is associated with a decrease in the F2-layer maximum electron density. In the longitude sector 80°–110° E (the zone of the East Siberian Continental Magnetic Anomaly), symmetrical to the geomagnetic pole located in the Western Hemisphere, the level of GMF variations is always low. In this regard, over Eurasia at longitudes ~80°–110°, the ionosphere has a stable positive anomaly and recovers first after geomagnetic disturbances (see Figure 2, *a*, *b*).

Another cause of the observed longitude variations in ionospheric parameters, especially in the high-latitude region, is the mismatch between the magnetic and geographical poles (the so-called UT effect) [Kolesnik, Golikov, 1982; Krinberg, Tashchilin, 1984; Deminov et al., 1992; Gololobov et al., 2014; Deminov, Shubin, 2018; Karpachev et al., 2019; Karpachev, 2021]. The amplitude of longitude variations in the electron density at high latitudes can be as high as an order of magnitude. The spatial structure of the high-latitude ionosphere is closely related to the magnetosphere and depends on the processes occurring in it, such as electric fields and precipitating charged particles. These processes are described in a geomagnetic coordinate system. Taking into account the UT effect leads to the fact that the regions of magnetospheric processes will shift relative to the terminator depending on universal time (UT). For example, magnetospheric convection, which at different moments of UT changes its location relative to the terminator due to the mismatch between Earth's rotation axis and the geomagnetic dipole axis, significantly affects the space-time distribution of the ionospheric electron density.

At subauroral latitudes, the mismatch between geographical and geomagnetic axes gives rise to a number of features of the formation of structures of ionospheric ionization troughs [Kolesnik, Golikov, 1982; Deminov et al., 1992; Gololobov et al., 2014; Deminov, Shubin, 2018; Karpachev et al., 2019; Karpachev, 2021]. These

are pronounced seasonal differences, as well as differences between western and eastern longitudes of the high-latitude ionosphere, consisting in the fact that western longitudes of the Northern Hemisphere are located closer to the geomagnetic pole than eastern longitudes. The main ionospheric trough (MIT), for instance, which is most pronounced in the nighttime F2-region in winter and represents a depression in the latitudinal electron density distribution located at geomagnetic latitudes 50°–70° N, exhibits a longitude dependence of the formation of spatial ionization irregularity. Kolesnik and Golikov [1982] showed that in winter in the Eastern Hemisphere if the geographic and geomagnetic poles in the subauroral ionosphere are mismatched, a region without effective sources of ionization is formed due to which MIT in the Eastern Hemisphere is deeper than in the Western Hemisphere. The trough manifests itself throughout the polar night unlike the Western Hemisphere where MIT is formed only at night.

The long-term effect of negative ionospheric disturbance during the recovery phase of magnetic storms is linked to disturbances in the form of thermospheric waves of molecular gas [Chernigovskaya et al., 2019, 2020, 2021, 2023, 2024]. This wave is generated in the lower thermosphere of polar latitudes in the nightside sector during a strong westward electrojet in the magnetic storm main phase. Due to the high rate of molecular ion-neutral collisions, this wave gains a large scale and momentum and moves southwestward over long distances even when the magnetospheric source is "turned off" in auroral latitudes.

An increase in the maximum electron density (f_oF2) at midlatitudes of the Northern Hemisphere over a vast region of Siberia and Europe after March 20 (Figure 2, *b, d*) with f_oF2 exceeding the level for quiet days (March 15–16) before the magnetic disturbance can be considered as a manifestation of the aftereffect of magnetic storms [Klimenko et al., 2018]. This effect manifests itself in the formation of positive electron density disturbances in the daytime a few days after the start of the magnetic storm recovery phase. The main cause of the observed positive electron density disturbances, according to [Klimenko et al., 2018; Ratovsky et al., 2018], is an increase in the atomic oxygen density due to its transfer from equatorial to middle latitudes in the late recovery phase. In turn, this transfer is driven by the additional pressure gradient of neutral gas from low to high latitudes, which arises from the appearance of excess neutral gas density at low latitudes in the geomagnetic storm main phase due to the transfer of oxygen from auroral latitudes to the equator. The authors compare the perturbation of [O]/[N_2] during and after the magnetic storm, as well as perturbation of the electron density, which passes from the negative phase to the positive one within a few days after the beginning of the magnetic storm recovery phase, with pendulum oscillations.

This aftereffect was especially pronounced in data from the ionosondes in Irkutsk and Novosibirsk from March 20 (Figures 2, *b*, 3, *b*). Recall that these ionosondes are located in the longitude sector 80°–110° E (the zone of the East Siberian Continental Magnetic Anomaly), where the level of GMF variations is always lower than in adjacent longitude regions. From March 21–22, the aftereffect was also observed in data from the European ionosondes in Ekaterinburg, Moscow, Průhonice, and Juliusruh (Figures 2, *b*, 3, *b*), as well as from GPS/GLONASS receivers (Figure 2, *d*). Thus, the effects in the F-region during the recovery phase of the magnetic storm in March 2015 (a strong decrease in the electron density followed by an increase) were detected initially for the ionosondes in the Far East and Eastern Siberia, later for the European ionosondes. This time sequence of the ionization effects also indirectly indicates that the ionization wave moves over Eurasia from east to west.

CONCLUSIONS

Studying the ionospheric response to the severe magnetic storm in March 2015 by analyzing data from ionosonde chains at high and middle latitudes of the Northern Hemisphere, as well as GUVI TIMED satellite measurements of the density ratio [O]/[N_2] in the thermospheric gas column above ~100 km, allows the following conclusions.

Joint study of longitude-time distributions of f_oF2, $f_o E_s$, and f_{min} based on data from VS ionosondes and TEC data from GPS/GLONASS receivers made it possible to carry out a comprehensive analysis of the ionospheric response at different altitude levels over Eurasia for different latitudes and longitudes during the severe geomagnetic disturbance.

The ionospheric response to the magnetic storm in March 2015 over Eurasia was observed with a change of the effect of the positive ionospheric storm immediately after the storm sudden commencement (SSC) on March 17 to the effect of the negative ionospheric storm in the second half of the day during the magnetic storm main phase. The transition from an increase in the maximum electron density to its sharp decrease was especially pronounced in the mid-latitude ionosphere. This scenario of the development of an ionospheric storm with a change of positive and negative effects is common for the equinoctial season.

During the magnetic storm main and recovery phases, there were periods of blackouts of ionosonde radio signals at high and middle latitudes. These periods of complete absence of signals during magnetic disturbances are associated with the joint action of mechanisms for decreasing the electron density in the upper ionosphere (negative ionospheric storms), abnormally increasing radio wave absorption in the lower ionosphere due to precipitation of energetic particles from the magnetosphere into the high-latitude ionosphere, as well as forming screening sporadic E_s layers. There were, for example, large gaps in f_oF2 data for the ionosondes in Salekhard, Lovozero, and Sodankylä on March 18–19. Complete radio signal blackouts occurred at night when the probability of formation of ionization troughs is high. On the same days, there was a noticeable increase in f_{min} and hence in radio wave absorption in the D-region, as well as in the rate of occurrence of E_s layers preventing upward propagation of radio signals.

We observed large latitude and longitude differences between features of time variations of the analyzed ionospheric parameters both under quiet conditions before the magnetic storm and during its development.

Noteworthy are the differences in the ionization of high and middle latitudes over Eurasia at the equinox both in the general level of ionization and in diurnal variations under quiet conditions (before the storm). With increasing geomagnetic activity in the conditions of the development of the ionospheric storm at high latitudes, a strong temporal variability was observed in the maximum electron density (f_oF2). Yet, the variability in f_oF2 for high-latitude ionosondes compared to daily average f_oF2 under quiet conditions on a relative scale is lower than the variability in f_oF2 at midlatitudes, even in the case of such a severe magnetic storm.

The ionospheric parameters according to data from VS ionosondes, located at approximately the same latitudes, show significant longitudinal differences. We have observed a very long period (almost until March 24) of decreased values of f_oF2 and hence of the electron density at the height of the F2-layer maximum, and at the same time increased f_{min} and f_oE_s, which suggest that the electron density is higher in the lower ionosphere in the D and E layers, as measured by the easternmost ionosondes: the high-latitude ionosonde in Pevek and the mid-latitude one in Paratunka. This indicates that the entire thickness of the high- and mid-latitude ionosphere over the Far Eastern region was disturbed during the main and recovery phases of the magnetic storm and for several more days after the end of the geomagnetic disturbance, although the ionosphere in the adjacent western regions of Eastern and Western Siberia had already returned to quiet conditions. The variability of the analyzed parameters on this time interval significantly differed from the daily average level in quiet conditions. All diurnal variations of f_oF2 were below the quiet level. Maximum daily (morning or afternoon) values of f_{min} exceeded quiet values by ~ 3 MHz (more than three times) for the mid-latitude ionosonde in Paratunka. According to data from the high-latitude ionosonde in Pevek, the increase in f_{min} was slightly smaller (about twice).

During the recovery phase of ionospheric ionization, the disturbances in the form of thermospheric waves of molecular gas propagating in a westerly direction for several days can play an important role in the dynamics of the ionosphere of high and especially middle latitudes. Motion of the region of the reduced density ratio [O]/[N_2] from the Far East and Siberia westward to the territory of Europe explains the long-term effect of the negative ionospheric storm over the high- and mid-latitude European regions until March 22–23 when the recovery phase of the magnetic storm had already ended.

An increase in the electron density in the ionosphere at midlatitudes of the Northern Hemisphere over a vast region of Siberia during the daytime after March 20, a little later over Europe with f_oF2 exceeding the level for quiet days before the magnetic disturbance can be considered as a manifestation of the aftereffect of magnetic storms. This effect was most pronounced in data from the ionosondes in Irkutsk, Novosibirsk from March 20, which are located in the longitude sector 80°–110° E (zone of the East Siberian Continental Magnetic Anomaly), where the level of GMF variations is always lower compared to adjacent longitude regions.

Taking into account the conclusions of this study, we once again call for a refinement of the traditional approach to the time interval of the analysis of the ionospheric effects of geomagnetic disturbances when the analysis ends at *Dst*–20 nT and the magnetospheric source of the disturbance is already "turned off" since the neutral gas composition disturbances launched during the development of the magnetic storm and resulting in electron density variations in the ionosphere may continue for several more days after the end of the magnetic storm.

The work was partially carried out with the financial support from the Ministry of Science and Higher Education of the Russian Federation; under the Project "Development and Modernization of Technologies for Monitoring Geophysical Conditions over the Territory of the Russian Federation and the Arctic"; the Ministry of Science and Higher Education of the Russian Federation (project FWZZ-2022-0019); IKIR FEB RAS assignment (State Registration Number in INIS RDE 124012300245-2). Experimental data was partially obtained using the equipment of Shared Equipment Center “Angara” (ISTP SB RAS) [http://ckp-rf.ru/ckp/3056]; as well as the Northeast Heliogeophysical Center CKP 558279, Unique Research Facility 351757 (IKIR FEB RAS).

Data from Sodankylä, Průhonice, and Juliusruh ionosondes were taken from the UK Solar System Data Center [https://www.ukssdc.ac.uk]).

The GUVI TIMED data used in this work is provided with the support of the NASA MO&DA program. The GUVI instrument was devised and built by the Aerospace Corporation and the Johns Hopkins University. The scientific supervisor is Larry J. Paxton.

REFERENCES

Araujo-Pradere E.A., Fuller-Rowell T.J., Codrescu M.V., Bilitza D. Characteristics of the ionospheric variability as a function of season, latitude, local time, and geomagnetic activity. *Radio Sci*. 2005, vol. 40, RS5009. DOI: 10.1029/2004RS003179.

Blagoveshchensky D.V., Maltseva O.A., Anishin M.M.,. Rogov D.D. Sporadic E_s layers at high latitudes during a magnetic storm of March 17, 2015 according to the vertical and oblique ionospheric sounding data. *Radiophysics and Quantum Electronics*. 2017, vol. 60, no. 06, pp. 456–466. DOI: 10.1007/s11141-017-9814-y.

Bryunelli B.E., Namgaladze A.A. *Fizika ionosfery* [*Physics of Ionosphere*]. Moscow, Nauka Publ., 1988, 527 p. (In Russian).

Buonsanto M.J. Ionospheric storms — a review. *Space Sci. Rev*. 1999, vol. 88, pp. 563–601.

Burešová D., Laštovička J., De Franceschi G. *Manifestation of Strong Geomagnetic Storms in the Ionosphere above Europe. Space Weather*. J. Lilensten (ed.), Springer. 2007, pp. 185–202.

Chernigovskaya M.A., Shpynev B.G., Khabituev D.S., Ratovskii K.G., Belinskaya A.Yu., Stepanov A.E., et al. Longitudinal variations of geomagnetic and ionospheric parameters during severe magnetic storms in 2015. *Sovremennye problemy distantsionnogo zondirovaniya Zemli iz kosmosa* [Current Problems in Remote Sensing of the Earth from Space]. 2019, vol. 16, no. 5, pp. 336–347. DOI: 10.21046/2070-7401-2019-16-5-336-347. (In Russian).

Chernigovskaya M.A., Shpynev B.G., Yasyukevich A.S., Khabituev D.S. Ionospheric longitudinal variability in the Northern Hemisphere during magnetic storm from the ionosonde and GPS/GLONASS data. *Sovremennye problemy distantsionnogo zondirovaniya Zemli iz kosmosa* [Current Problems in Remote Sensing of the Earth from Space].. 2020, vol. 17, no. 4, pp. 269–281. DOI: 10.21046/2070-7401-2020-17-4-269-281. (In Russian).

Chernigovskaya M.A., Shpynev B.G., Yasyukevich A.S., Khabituev D.S., Ratovsky K.G., Belinskaya A.Yu., Stepanov A.E., et al. Longitudinal variations of geomagnetic and ionospheric parameters in the Northern Hemisphere during magnetic storms according to multi-instrument observations. *Adv. Space Res*. 2021, vol. 67, no. 2, pp. 762–776. DOI: 10.1016/j.asr.2020.10.028.

Chernigovskaya M.A., Yasyukevich A.S., Khabituev D.S. Ionospheric longitudinal variability in the Northern Hemisphere during magnetic storms in March 2012 from ionosonde and GPS/GLONASS data. *Solar-Terr. Phys*. 2023, vol. 9, iss. 4, pp. 99–110. DOI: 10.12737/stp-94202313.

Chernigovskaya M.A., Setov A.G., Ratovsky K.G., Kalishin A.S., Stepanov A.E. Variability of ionospheric ionization over Eurasia according to data from a high-latitude ionosonde chain during extreme magnetic storms in 2015. *Solar-Terr. Phys*. 2024, vol. 10, iss. 2, pp. 34–47. DOI: 10.12737/stp-102202404.

Christensen A.B., Paxton L.J., Avery S., Craven J., Crowley G., Humm D.C., et al. Initial observations with the Global Ultraviolet Imager (GUVI) on the NASA TIMED satellite mission. *J. Geophys. Res*. 2003, vol. 108, no. A12, p. 1451. DOI: 10.1029/2003JA009918.

Danilov A.D. Long-term trends of f_0F2 independent on geomagnetic activity. *Ann. Geophys*. 2003, vol. 21, no. 5, pp. 1167–1176.

Deminov M.G. Earth's ionosphere: patterns and mechanisms. *Electromagnetic and plasma processes from the interior of the Sun to the interior of the Earth*. *IZMIRAN-75*. Moscow, 2015, pp. 295–346. (In Russian).

Deminov M.G., Shubin V.N. Empirical model of the location of the main ionospheric trough. *Geomagnetism and Aeronomy*. 2018, vol. 58, no. 3, pp. 348–355. DOI: 10.1134/S0016793218030064.

Deminov M.G., Karpachev A.T., Afonin V.V., Smilauer J. Changes in the position of the main ionospheric trough as a function of longitude and geomagnetic activity. *Geomagnetism and.Aeronomy*. 1992, vol. 32, no. 5, pp. 185–188. (In Russian).

Gololobov A.Yu., Golikov I.A., Popov V.I. Modeling of the high-latitude ionosphere taking into account the mismatch of the geographic and geomagnetic poles. *Vestnik of North-Eastern Federal University*. 2014, vol. 11, no. 2, pp. 46–54. (In Russian).

Enell C.-F., Kozlovsky A., Turunen T., Ulich T., Välitalo S., Scotto C., Pezzopane M. Comparison between manual scaling and Autoscala automatic scaling applied to Sodankylä Geophysical Observatory ionograms. *Geosci. Instrum. Method. Data Syst*. 2016, no. 5, pp. 53–64. DOI: 10.5194/gi-5-53-2016.

Hunsucker R.D., Hargreaves J.K. *The High-Latitude Ionosphere and its Effects on Radio Propagation*. Cambridge University Press, New York, 2003, 617 p.

Kalishin A.S., Blagoveshchenskaya N.F., Troshichev O.A., Frank-Kamenetskii A.V. FGBU «AARI». Geophysical research in high latitudes. *Vestnik RFFI. Antarktida i Arktika: Polyarnye issledovaniya* [RFBR J. Antarctica and Arctic: Polar Research]. 2020, no. 3-4 (107–108), pp. 60–74. DOI: 10.22204/2410-4639-2020-106-107-3-4-60-78. (In Russian).

Karpachev A.T. Model of the ionospheric trough for daytime winter conditions based on data from Interkosmos-19 and champ satellites. *Geomagnetism and Aeronomy*. 2019, vol. 59, pp. 383–397. DOI: 10.1134/S0016793219040091.

Karpachev A.T. Dynamics of main and ring ionospheric troughs at the recovery phase of storms/substorms. *J. Geophys. Res*. 2021, vol. 126, e2020JA028079. DOI: 10.1029/2020JA 028079.

Karpachev A.T., Klimenko M.V., Klimenko V.V. Longitudinal variations of the ionospheric trough position. *Adv. Space Res*. 2019, vol. 63, iss. 2, pp. 950–966. DOI: 10.1016/j.asr.2018.09.038.

Klimenko M.V., Klimenko V.V., Despirak I.V., Zakharenkova I.E., Kozelov B.V., Cherniakov S.M., Andreeva E.S., et al. Disturbances of the thermosphere–ionosphere–plasmasphere system and auroral electrojet at 30° E longitude during the St. Patrick's Day geomagnetic storm on 17–23 March 2015. *J. Atmos. Solar-Terr. Phys*. 2018, vol. 180, pp. 78–92. DOI: 10.1016 /j.jastp.2017.12.017.

Kolesnik A.G., Golikov I.A. Three-dimensional model of the high-latitude region F, taking into account the discrepancy between geographical and geomagnetic coordinates). *Geomagnetism and Aeronomy*. 1982, vol. 22, no. 3, pp. 435–439. (In Russian).

Kozlovsky A., Turunen T., Ulich T. Rapid-run ionosonde observations of traveling ionospheric disturbances in the auroral ionosphere. *J. Geophys. Res*. 2013, vol. 118, pp. 5265–5276.

Krasheninnikov I., Pezzopane M., Scotto C. Application of Autoscala to ionograms recorded by the AIS-Parus ionosonde. *Computers & Geosciences*. 2010, vol. 36, pp. 628–635. DOI: 10.1016/j.cageo.2009.09.013.

Krinberg I.A., Tashchilin A.V. *Ionosphere and Plasmasphere*). M.: Nauka, 1984, 188 p. (In Russian).

Laštovička J. Monitoring and forecasting of ionospheric space weather effects of geomagnetic storms. *J. Atmos. Solar-Terr. Phys*. 2002, vol. 64, pp. 697–705. DOI: 10.1016/S1364-6826(02)00031-7.

Liou K., Newell P.T., Anderson B.J., Zanetti L., Meng C.-I. Neutral composition effects on ionospheric storms at middle and low latitudes. *J. Geophys. Res*. 2005, vol. 110, p. A05309. DOI: 10.1029/2004JA010840.

Loewe C.A., Prölss G.W. Classification and mean behavior of magnetic storms. *J. Geophys. Res*. 1997, vol. 102, no. A7, pp. 14,209–14,213.

MacDougall J.W., Grant I.F., Shen X. The Canadian advanced digital ionosonde: design and results. *WDC A for Solar-Terrestrial Physics, Report UAG-104*, Boulder, Colorado, USA. 1995, pp. 21–27.

Mamrukov A.P., Khalipov V.L., Filippov L.D., Stepanov A.E., Zikrach EH.K., Smirnov V.F., Shestakova L.V. Geophysical information on oblique radio reflections at high latitudes and their classification). *Issledovaniya po geomagnetizmu, aehronomii i fizike Solntsa* [Research on Geomagnetism, Aeronomy and Solar Physics]. Novosibirsk, SB RAS Publ. 2000, vol. 111, pp. 14–27. (In Russian).

Matsushita S. A study of the morphology of ionospheric storms. *J. Geophys. Res*. 1959, vol. 64, no. 3, pp. 305–321. DOI: 10.1029/JZ064i003p00305.

Mikhailov A.V. Ionospheric F2-layer storms. *Física de la Tierra*. 2000, vol. 12, pp. 223–262.

Mitra A. *Impact of solar flares on the Earth's ionosphere*. Moscow, Mir Publ., 1977, 372 p. (In Russian).

Perevalova N.P., Ratovsky K.G., Zherebtsov G.A., Yasyukevich A.S. Correlation of short-period wave disturb-

ances of the peak electron density of the F2 layer and the total electron content in the ionosphere. *Doklady Earth Sciences*, 2023, vol. 513, no. 1, pp. 1194–1199. DOI: 10.1134/S1028334X2360192X.

Polyakov V.M., Shchepkin L.A., Kazimirovsky E.S., Kokourov V.D. *Ionospheric processes*. Novosibirsk: Nauka, 1968, 535 p. (In Russian).

Prölss G.W., Werner S. Vibrationally excited nitrogen and oxygen and the origin of negative ionospheric storms. *J. Geophys. Res*. 2002, vol. 107, no. A2, p. 1016. DOI: 10.1029/2001JA900126.

Ratovsky K.G., Klimenko M.V., Klimenko V.V., Chirik N.V., Korenkova N.A., Kotova D.S., Aftereffects of geomagnetic storms: statistical analysis and theoretical explanation. *Solar-Terr. Phys*. 2018, vol. 4, no. 4, pp. 26–32. DOI: 10.12737/stp-44201804.

Ratovsky K.G., Klimenko M.V., Yasyukevich Y.V., Klimenko V.V., Vesnin A.M. Statistical analysis and interpretation of high-, mid-and low-latitude responses in regional electron content to geomagnetic storms. *Atmosphere*. 2020, vol. 11, no. 12, p. 1308. DOI: 10.3390/atmos11121308.

Reinisch B.W., Haines D.M., Bibl K., Galkin I., Huang X., Kitrosser D.F., Sales G.S., Scali J.L. Ionospheric sounding support of OTH radar. *Radio Sci*. 1997, vol. 32, no. 4, pp. 1681–1694.

Tumanova Yu.S., Andreeva E.S., Nesterov I.A. Observations of an ionospheric trough over Europe at different levels of geomagnetic disturbance based on radio tomography data. *Uchenye zapiski fizicheskogo fakul'teta MGU* [Memoirs of the Faculty of Physics, Lomonosov Moscow State University]. 2016, no. 3, 163906. (In Russian).

Vystavnoy V.M., Makarova L.N., Shirochkov A.V., Egorova L.V. Investigations of the high-latitude ionosphere by using data of the modern digital vertical ionosonde CADI, *Geliogeofizicheskie issledovaniya*, 2013, Vol. 4, pp. 1–10 (in Russian).

URL: https://www.swpc.noaa.gov/noaa-scales-explanation (accessed April 22, 2024).

URL: http://ckp-rf.ru/ckp/3056/ (accessed April 22, 2024).

URL: https://www.ukssdc.ac.uk (accessed April 22, 2024).

Original Russian version: Chernigovskaya M.A., Ratovsky K.G., Zherebtsov G.A., Setov A.G., Khabituev D.S., Kalishin A.S., Stepanov A.E., Belinskaya A.Yu., Bychkov V.V., Grigorieva S.A., Panchenko V.A., published in Solnechno-zemnaya fizika. 2024. Vol. 10. No. 4. P. 51–64. DOI: 10.12737/szf-104202406.

How to cite this article

Chernigovskaya M.A., Ratovsky K.G., Zherebtsov G.A., Setov A.G., Khabituev D.S., Kalishin A.S., Stepanov A.E., Belinskaya A.Yu., Bychkov V.V., Grigorieva S.A., Panchenko V.A. Ionospheric response over the high and middle latitude regions of Eurasia according to ionosonde data during the severe magnetic storm in March 2015. *Solar-Terrestrial Physics*. 2024. Vol. 10. Iss. 4. P. 46–58. DOI: 10.12737/stp-104202406.